

FD 177: Negative Hyperconjugation and Red-, Blue- or Zero-Shift in X-Z---Y Complexes

Journal:	<i>Faraday Discussions</i>
Manuscript ID:	FD-ART-09-2014-000183.R1
Article Type:	Paper
Date Submitted by the Author:	09-Nov-2014
Complete List of Authors:	Jemmis, Eluvathingal; Indian Institute of Science, Department of Inorganic and Physical Chemistry Jyothish, Joy; Indian Institute of Science Education and Research Thiruvananthapuram, School of Chemistry Kaipanchery, Vidya; Indian Institute of Science Education and Research Thiruvananthapuram, Chemistry

Negative Hyperconjugation and Red-, Blue- or Zero-Shift in X-Z---Y Complexes.

Jyothish Joy,^a Eluvathingal D. Jemmis,^{*b} and Kaipanchery Vidya^a

DOI: 10.1039/b000000x [DO NOT ALTER/DELETE THIS TEXT]

5 A generalized explanation is provided for the existence of red- and blue-
shifting nature of the X-Z bonds (Z = H, Halogens, Chalcogens, Pnicogens,
etc.) in X-Z---Y complexes based on computational studies on a selected
set of weakly bonded complexes and analysis of existing literature data.
The additional electrons and orbitals available on Z in comparison to H
10 make for dramatic differences between H-Bond and rest of the Z-Bonds.
The nature of X-group and its influence on the X-Z bond length in the
parent X-Z molecule largely controls the change in the X-Z bond length on
X-Z---Y bond formation; the Y-group usually influences only the
magnitude of the effects controlled by the X. The major factors which
15 control the X-Z bond length change are: (a) negative hyperconjugative
donation of electron density from X-group to X-Z σ^* antibonding
molecular orbital (ABMO) in the parent X-Z, (b) induced negative
hyperconjugation from the lone pair of electrons on Z to the antibonding
orbitals of the X-group, and (c) charge transfer (CT) from Y-group to the
20 X-Z σ^* orbital. The exchange repulsion from Y-group that shifts partial
electron density at the X-Z σ^* ABMO back to X leads to blue-shifting and
the CT from the Y-group to the σ^* ABMO of X-Z leads to red-shifting. The
balance between these two opposing forces decides red-, zero- or blue-
shifting. A continuum of behaviour of X-Z bond length variation is
25 inevitable in X-Z---Y complexes.

1. Introduction

Early stages of the studies of weak interactions in chemistry were dominated by the
H-Bond due to its obvious importance in Biology.^{1, 2} Detailed understanding of the
nature, variety and mechanism of X-H---Y interactions, where X is an atom or
30 molecular fragment and Y is an atom or molecule, has led to many novel ideas in
weak interactions. The inevitability of H-Bond in all branches of Chemistry is now
known and its detailed understanding has helped to bring new perceptions to the
research in Material Science and Crystal Engineering.^{3, 4} Weak interactions akin to
H-bond must exist for any element in the periodic table in appropriate molecular
35 combinations. Indeed, several examples have appeared in the past for weak

^a School of Chemistry, Indian Institute of Science Education and Research-Thiruvananthapuram,
Thiruvananthapuram, Kerala, 695016, India.

^b Department of Inorganic and Physical Chemistry, Indian Institute of Science, Bangalore,
40 560012, India. Fax: 2360-1552; Tel: 080-2293-3347; E-mail: jemmis@ipc.iisc.ernet.in

† Electronic Supplementary Information (ESI) available: Coordinates of the model complexes and
evidence for Proper and Pro-improper nature of model systems. See DOI: 10.1039/b000000x/

interactions involving elements other than hydrogen.⁵ While the formulation X-Z---Y for these interactions and the name Z-bond where the Z is any atom, with or without further substituents, brings the similarity to the H-Bond and the X-H---Y interaction, major additional factors are expected to play important role in the Z-Bonds. Halogen bonds,⁶⁻⁸ Chalcogen bonds,^{9, 10} Pnicogen bonds,^{11, 12} Tetral bonds¹³⁻¹⁵ and others have far more flexibility than the H-Bond as the H atom with its one electron and one valence orbital is unique. Additionally the unit mass of H which is invariably several times lighter than X lends X-H bond tractable by variations in the X-H stretching frequency. We are particularly interested to understand the blue- and red- shifting in X-Z bond and contrast these with the H-Bonds. On the other hand, pure X-Z stretching modes are rare.^{6, 16-18} This forces us to depend on the X-Z bond length rather than its stretching frequency.

Various explanations had been given by different groups of investigators for the red- and blue-shifting nature of hydrogen bond.¹⁹⁻²⁵ A few years ago we examined these aspects in detail and proposed a unified explanation for the nature of X-H bond length variation based on the change in electron density.²⁶ We had shown that there is nothing “improper” or “anti” about the blue-shifting H-bonds and that all are a part of the continuum of behaviour.^{27, 28} Using the terminology prevalent at that time we had classified the H-bonds as Proper, Pro-improper and Improper based on the X-H bond length and vibrational frequency change during the complex formation. Proper H-bonds show an increase in X-H bond length and decrease in vibrational frequency (red-shifting) while X-H and Y are brought to form X-H---Y complex. Pro-improper H-bonds may be red- or blue-shifting, but show an initial X-H bond length contraction and increase in vibrational frequency (blue-shifting) at large donor-acceptor separation and, finally leads to red-shifting or blue-shifting at equilibrium geometry. Improper H-bonds have blue-shift in the X-H stretching frequency from larger intermolecular distances itself as the X-H and Y are brought together. A similar understanding is possible for Z-bonds in the X-Z---Y interaction. Red- and blue-shifting X-Z bonds in X-Z---Y interaction, especially in Halogen bonds (Z=Halogen) have been studied by many groups in recent years, but detailed analysis and general explanations that can be transferred to other examples are not available. Apart from a charge analysis, previous studies did not concentrate on the influence of the starting X-Z distance (brought in by the X group in the monomer X-Z) on the nature of blue- and red- shifting in X-Z---Y complex.⁷ Studies on the weak X-Z---Y bonds where Z= Chalcogen,^{9, 10} Pnicogen,^{11, 12} Carbon¹³⁻¹⁵ are evolving, but none has yet focussed on the continuum nature of the red- and blue-shifting X-Z bonds in the X-Z---Y. The X-group plays an important role in deciding the nature of X-Z bond length variation during the complex formation, much more than what is possible in the H-Bond and hence a detailed analysis of the mechanism is necessary.

The present study focuses on the detailed explanation about the continuum nature of red- and blue-shifting X-Z bonds in any X-Z---Y complex, using model complexes FCl, CF₃Cl and NO₂Cl as X-Z and NH₃ as Y. A generalized concept of X-Z bond length change in any weakly interacting complex based on the relative competition between negative hyperconjugation in the donor molecule and charge transfer (CT) from the incoming acceptor molecule evolves from this study. The additional electrons and orbitals available on Z in comparison to H make for dramatic differences between H-Bond and rest of the Z-Bonds.

2. Computational Details

The three model systems under detailed investigation are calculated at *ab-initio* second order Møller-Plesset theory (MP2). All the geometries are optimized at MP2(full)/aug-cc-pVTZ level of theory without any constraints and are verified to be ground state by frequency calculations using Gaussian09 quantum chemistry package.²⁹ This level of theory and basis set are reported to give relatively good results for weak interactions.^{30, 31} Double Hybrid functional with Grimmes third order dispersion correction,^{32, 33} B2PLYP-D3 was also used to check the reliability of calculations and the results are found to be in good agreement with the MP2 results. Errors due to basis set superposition (BSSE) are corrected using the standard Counter Poise (CP) correction method of Boys and Bernardi.³⁴ Electron Density analysis were performed using ADF2013.01 DFT package³⁵ and AIM2000 suite of programs.³⁶ Deformation density plots, which give information about the extent of electron density reorganization during the complex formation, are obtained using ETS-NOCV^{37, 38} method implemented in ADF2013.01. Wavefunction files required for AIM analysis were generated from MP2 calculations. Population analysis, partial atomic charges and charge transfer analysis on MP2 optimized geometries are done by standalone NBO6 program³⁹ at M06-2x/aug-cc-pVTZ level of theory using Gaussian09 as the ESS host package. Most of the complexes analysed to establish the continuum nature are well known and are available in the literature. We have re-computed these geometries at MP2(full)/6-311+g(d,p) level of theory to substantiate the proposed hypothesis (Supporting Materials).

While going from H-bond to the Z-bond, we realize that the variation in the stretching frequency is no longer the most suitable parameter to represent bond strength for the following reason. In the X-H bond, it is almost always possible to get a pure X-H stretching frequency. However, heavier Z-atoms have several of the vibrational modes mixing with the X-Z stretching mode, so that an accurate estimate of blue- and red-shifting is not easily possible.^{6, 16-18} Therefore we rely largely on bond length variation as an indicator of bond strength and red-, zero- or blue-shift in the X-Z stretch.

3. Results and Discussions

We have performed detailed theoretical analysis on three selected halogen bonded systems, F-Cl---NH₃ (red-shifted), F₃C-Cl---NH₃ (moderately blue-shifted) and O₂N-Cl---NH₃ (strongly blue-shifted). These structures are optimized by keeping the Z---Y distance at several selected values by scanning the potential energy surface. The well-established idea of charge transfer (CT) from the acceptor group (Y) to the X-Z σ^* anti-bonding molecular orbital (ABMO) of the donor as the reason for bond length elongation (red-shift), prompts us to speculate the situation where X-Z σ^* ABMO is already occupied at the monomer level. What will happen if electron rich Y-group approach such an X-Z molecule? Our analysis depends on the variation of several parameters as a function of the Z---Y distance, through a series of scan calculations. The following parameters are especially analysed as a function of Z---Y distance: a) total energy; b) X-Z bond length; c) variation of the occupancy of the X-Z σ^* ABMO; d) charge transfer from Y to X-Z; e) negative hyperconjugation from X to Z and from Z to X; f) atomic population density; g) electron density at bond critical points for X-Z and Z---Y bonds; and h) deformation density at

equilibrium geometry.

3.1 Geometrical parameters and properties of the studied molecules

Table 1 Geometric parameters of the studied complexes at the equilibrium geometry. B.E = Binding Energy. ZPE = Zero Point Energy. BSSE = Basis Set Superposition Error. Calculations are done at MP2(full)/aug-cc-pVTZ level of theory.

Complex	d(Hal---Y) (Å)	$\Delta(X\text{-Hal})$ (Å)	$\langle(X\text{-Hal---Y})$ (degree)	B.E _{ZPE} (kcal/mol)	B.E _{ZPE-BSSE} (kcal/mol)
F-Cl---NH ₃	2.207	+0.0786	180.00	10.44	8.52
F ₃ C-Cl---NH ₃	3.041	-0.0064	179.96	2.31	1.78
O ₂ N-Cl---NH ₃	2.730	-0.0497	179.94	3.06	2.20

The scan calculations along the Cl---N distance between the donor and the acceptor molecules ranged from 6.0Å to 2.0Å with step size of 0.2Å. Except for this distance all other parameters are completely optimized for all separate values of Cl---N. The plots of X-Cl bond length and total energy against the scan coordinate are shown in Fig.1. Complex F-Cl---NH₃ (Fig. 1A) shows red-shift, complexes F₃C-Cl---NH₃ (Fig.1B) and O₂N-Cl---NH₃ (Fig.1C) show blue-shift compared to the free monomers. The highly blue-shifted O₂N-Cl---NH₃ complex shows drastic change in N-Cl bond length as compared to the other two systems and this behaviour seems to be highly abnormal. While the attractive interaction between monomers is justified in terms of the long range electrostatic attraction between sigma-hole on halogen and the electron density in Y (NH₃) group,⁴⁰⁻⁴² the details of the electron reorganization that causes this has to be analysed.

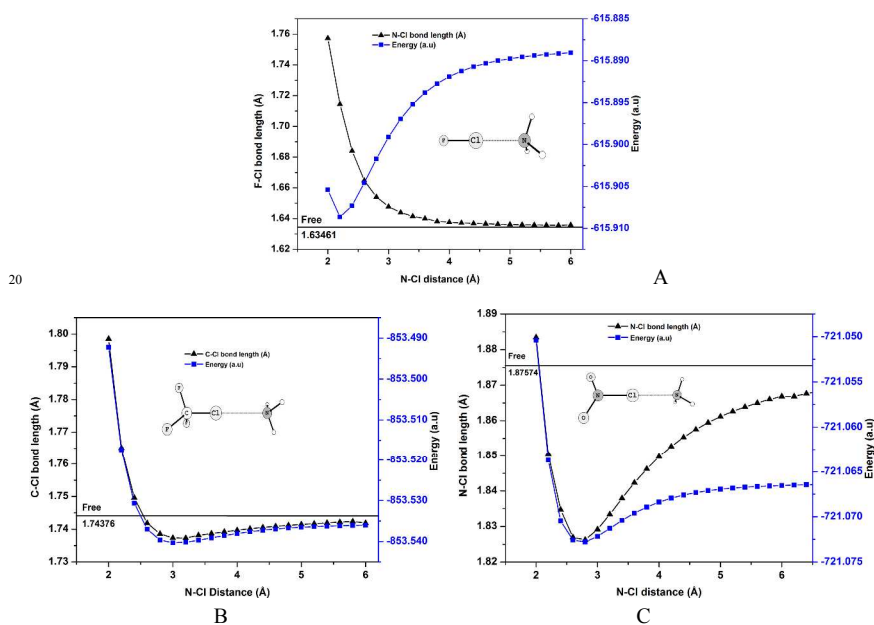


Fig. 1 Variation of X-Cl bond length and the total energy during the potential energy scan: (A) F-Cl---NH₃ (B) F₃C-Cl---NH₃ (C) O₂N-Cl---NH₃. Calculations are done at MP2(full)/aug-cc-pVTZ level of theory.

Electrostatic attraction between the σ -hole on the donor and electron density on the acceptor nitrogen is the primary reason for the interaction between monomers at larger separations. Nevertheless, complex (A) becomes red shifted and complex (B) and (C) becomes blue-shifted. Different authors give different explanations for this unusual behaviour. We believe that the factors that controls both red and blue-shifting in X-Z bond length exists in all complexes, except that these factors contribute in different magnitudes in different complexes. It is clear from the available literature that F-Cl belongs to the Proper category (pure red-shifting) of Z-Bond donors and there is no example of a blue-shifted F-Cl---Y complex. F_3C-Cl and O_2N-Cl belongs to the Pro-improper category of weak interactions, where red- or blue-shifting results depending on the nature of incoming Y-group. We propose that, it is the modulation of the already existing negative hyperconjugative donation of electron density from X-group to the X-Z σ^* ABMO in the monomer by the incoming Z-bond acceptor that makes for the pro-improper behaviour of X-Z bond. Negative hyperconjugation^{43, 44} is defined as the donation of electron density from the filled lone pair or p-orbital to the neighbouring σ^* orbital which is ant-periplanar to the donor orbital. The immediate consequence of this effect is an elongation of neighbouring bond which receives the electron density to its antibonding molecular orbital.

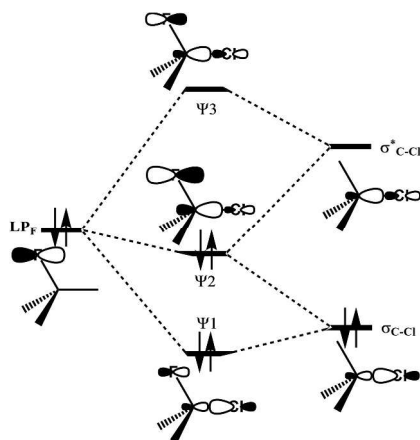


Fig. 2 Interaction diagram showing the negative hyperconjugative donation of F-lone pair (LP_F) to the C-Cl σ^* bond orbital in F_3C-Cl molecule.

The negative hyperconjugative donation of electron density from F atom to the C-Cl σ^* ABMO of F_3C-Cl molecule is shown in Fig. 2. Same interaction is possible for the lone pair on Cl atom to the C-F σ^* ABMO also. We do not anticipate any Fluorine-bonds in F_3CCl molecule because the positive electrostatic potential over Fluorine atom is not strong enough to interact with NH_3 molecule. Hence we only consider the donation of electron density from F atoms of $-CF_3$ group to the σ^* C-Cl bond. The extra electron density at the ABMO makes C-Cl bond elongated and it also decreases the electron density around Cl atom because of its synergic donation to C-F σ^* orbital. Bond orbitals participating in negative hyperconjugation and hyperconjugation (CT) in $F_3C-Cl---NH_3$ complex are shown in Fig. 3.

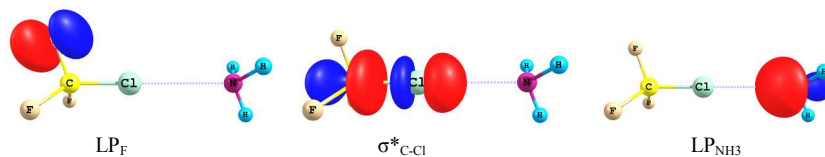


Fig. 3 NBO bond orbitals of $F_3C-Cl \cdots NH_3$ complex: LP_F donates to the σ^*_{C-Cl} (negative hyperconjugation). The CT at short distances takes place from the LP_{NH_3} to σ^*_{C-Cl} , often termed as hyperconjugation.[#] Calculations are done at MP2(full)/aug-cc-pVTZ level of theory.

In proper X-Z bonds, where negative hyperconjugation from X-group is absent, σ^* X-Hal orbital is vacant in the monomer and increases its occupancy during complex formation through charge transfer from Y group. This increases X-Hal bond length (red shifting). X-Hal bond will be highly elongated at the monomer level itself in systems where negative hyperconjugation is strong due to the presence of electrons in σ^* ABMO. Any incoming Y-group can perturb these extra electrons through long range exchange repulsion. This leads to the back flow of electron density from partially occupied σ^* ABMO of X-Hal bond to other parts of the molecule i.e., towards the X-group. This effect of back flow has two consequences: (i) extra electron density flows back from anti-bonding molecular orbital leading to bond length contraction (ii) electron density shift to the X-group makes it more negatively charged and connected halogen atom becomes more positively charged. The combined effect of electron density decrease at the σ^* orbital, and an increase in opposite charges in X-group and Halogen atom makes X-Hal bond shorter (blue-shifting). The possibility for charge transfer interactions in blue-shifted systems cannot be neglected. This is the reason why some of the systems which initially show preference towards blue-shifting become red-shifting at the equilibrium geometry (pro-improper). Hence the preference towards resultant red- or blue-shift in geometry is decided by the balance between negative hyperconjugation and charge transfer. Observations made by Hobza et al.^{19, 21} about blue-shift in hydrogen bonding is in line with our arguments, where they observed the flow of electron density through charge transfer to various parts of the donor molecule, apart from X-H σ^* ABMO orbital. The source of electron density involved in this process has to be evaluated in each case. As the shift of electron density begins even when the Y group is at 5.0Å (Fig. 1B and 1C), this is not caused by the additional electron density resulting from CT from the lone pair on Y. This is the long range effect of the Y group on the electron density at the X-Z bond. Careful analysis of dimer geometries obtained at each scan steps gives evidences for the existence of the proposed mechanism.

3.2 Negative hyperconjugation and σ^* occupancy of X-Hal bond

The effect of negative hyperconjugation on X-Hal bond length can be well demonstrated by analysing the σ^* ABMO occupancy. Let us consider the examples of O_2N-Cl and O_2NO-Cl ⁴⁵ as halogen bond donors. Here O_2N-Cl has reasonably high electron occupancy at the N-Cl σ^* ABMO but O-Cl in O_2NO-Cl has no σ^* occupancy from negative hyperconjugation. This makes O_2N-Cl , blue-shifting (-0.0497Å) as electron density can be shifted away from the σ^* ABMO and O_2NO-Cl red shifting (+0.0454Å) as the major contribution from CT to the σ^* ABMO during complex formation with NH_3 (Fig. 4).

This is not strictly hyperconjugation, which represents a delocalization involving pi-type and sigma type orbitals, but frequently used in this context.

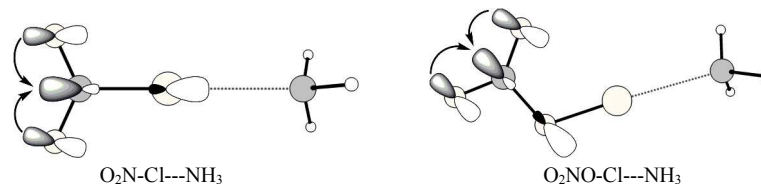
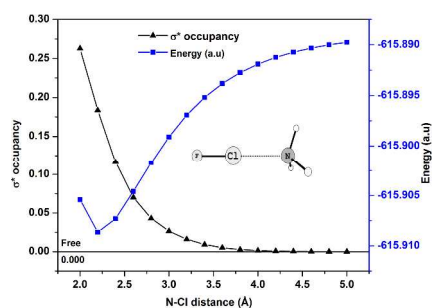


Fig. 4 Presence of negative hyperconjugative donation to N-Cl σ^* orbital in $\text{O}_2\text{N-Cl}\cdots\text{NH}_3$ and its absence in O-Cl σ^* orbital in $\text{O}_2\text{NO-Cl}\cdots\text{NH}_3$.

10 Plots of X-Hal σ^* orbital occupancy and total energy of the studied complexes against the scan coordinates (Fig. 5) support these ideas. The occupancy of the σ^* F-Cl increases as NH_3 approaches (Fig. 5A). The absence of negative hyperconjugation in F-Cl molecule leaves F-Cl σ^* orbital vacant and CT from NH_3 leads to bond length elongation (red shift). Complex $\text{O}_2\text{N-Cl}\cdots\text{NH}_3$ (Fig. 5 C) shows
 15 pure blue-shifting where σ^* occupancy decreases drastically during the approach of NH_3 through long range exchange repulsion and it shows minimum occupancy at equilibrium geometry and hence bond length contraction. Complex (B) is a mixture of both the effects operating in complex (A) and (C), where σ^* occupancy decreases to a minimum and bond contracts at the first stage but at equilibrium geometry
 20 (3.04 Å) occupancy slightly increases from minimum due to the presence of CT from NH_3 lone pair, Table 2. Hence complex (B) shows only a slight blue-shift because of the balance between CT and negative hyperconjugation. The balance between these two opposing forces and the equilibrium distance is to be contrasted with the thick horizontal line, which shows the bond occupancy in the monomer
 25 (Fig. 5). This, in turn, reflects the extend of the occupancy of X-Hal σ^* orbital. This is a handle for designing red- and blue-shifting bonds in any weakly interacting complexes. It is possible to tune the Y-group to force $\text{F}_3\text{C-Cl}$ to form a red-shifting complex. Hence there is a strong correlation between σ^* occupancy and the nature of the X-Z Bond in deciding the bond length variations in the X-Z---Y complex. Higher
 30 the σ^* occupancy in the monomer X-Z bond, greater will be the chance for blue-shifting.



A

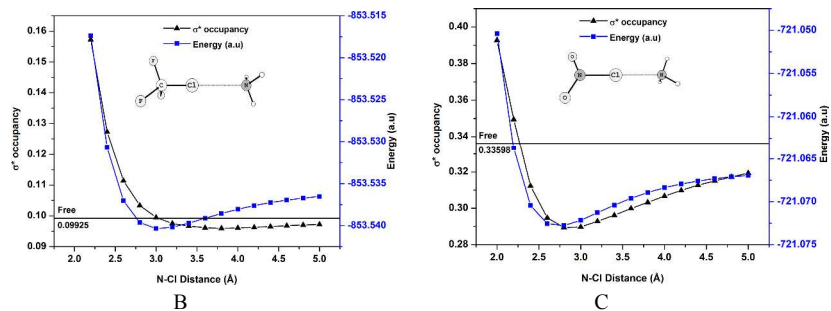


Fig. 5 Variation of X-Cl σ^* bond occupancy and total energy during the potential energy scan: (A) F-Cl---NH₃ (B) F₃C-Cl---NH₃ (C) O₂N-Cl---NH₃. Calculations are done at M06-2x/aug-cc-pVTZ level of theory.

Table 2 X-Cl σ^* occupancy of monomer, dimer and the resultant charge transfer (CT) from NH₃. Calculations are done at M06-2x/aug-cc-pVTZ level of theory.

Complex	Monomer σ^* occupancy	Dimer σ^* occupancy	CT	σ^* occupancy in the absence of CT
FCl---NH ₃	0.0000	0.1809	0.1772	0.0037
F ₃ CCl---NH ₃	0.0992	0.0990	0.0080	0.0910
O ₂ NCl---NH ₃	0.3359	0.2903	0.0267	0.2636

Table 3 NBO second order perturbation analysis (kcal/mol) showing hyperconjugation (CT) and negative hyperconjugation (NHC) at each of the scan geometries along with change in X-Hal bond length during the formation of X-Hal---Y. Values at equilibrium geometries are shown in bold numbers. Calculations are done at M06-2x/aug-cc-pVTZ level of theory.

Hal---Y (Å)	FCl---NH ₃			F ₃ C-Cl---NH ₃				O ₂ N-Cl---NH ₃			
	CT ^a	NHC ^b	Δ F-Cl	CT ^c	NHC ^d	NHC ^e	Δ C-Cl	CT ^f	NHC ^g	NHC ^h	Δ N-Cl
2.2	53.69	0.00	+0.079	31.13	11.70	9.66	+0.021	53.93	42.25	14.11	-0.025
2.4	27.71	0.00	+0.049	16.20	12.29	10.46	+0.006	29.12	41.89	16.71	-0.041
2.6	14.43	0.00	+0.030	8.78	12.71	11.03	-0.002	15.83	44.73	17.98	-0.049
2.8	7.89	0.00	+0.019	4.88	12.98	11.28	-0.005	8.97	47.31	18.46	-0.049
3.0	4.39	0.00	+0.013	2.79	13.29	11.23	-0.006	5.20	49.52	18.48	-0.047
3.2	2.42	0.00	+0.009	1.56	13.44	10.81	-0.006	2.99	51.44	18.31	-0.042
3.4	1.30	0.00	+0.007	0.86	13.63	10.15	-0.005	1.68	52.96	18.04	-0.038
3.6	0.67	0.00	+0.005	0.45	13.72	10.03	-0.005	0.92	54.24	17.74	-0.033
3.8	0.34	0.00	+0.004	0.23	13.77	9.00	-0.005	0.49	55.24	17.46	-0.029
4.0	0.17	0.00	+0.003	0.12	13.88	8.37	-0.004	0.25	56.12	17.21	-0.026

^a [L.P_{NH3} → σ^* _{F-Cl}]. ^b No NHC. ^c [L.P_{NH3} → σ^* _{C-Cl}], Fig.3. ^d [L.P_F → σ^* _{C-Cl}], Fig.3. ^e [L.P_{Cl} → σ^* _{C-F}]. ^f [L.P_{NH3} → σ^* _{N-Cl}]. ^g [L.P_O → σ^* _{N-Cl}]. ^h [L.P_{Cl} → π^* _{N-O}].

NBO second order perturbation analysis (Table 3) gives information about CT

from Y group and strength of negative hyperconjugation from X-group to the X-Hal σ^* ABMO. For pure red shifting cases, there is no negative hyperconjugation and hence X-Z bond length elongates always. In the case of complex (B) and (C) both negative hyperconjugation and CT are active. Negative hyperconjugation dominates at larger monomer separations and decreases as Y-group approaches and CT shows the opposite trend. The CT starts only below 3.5 Å of Hal---Y separation and hence we can conclude that any bond length change that occurs beyond 3.5 Å is purely due to the effect of long range exchange repulsion of Y-group on σ^* ABMO electron density. The decrease in negative hyperconjugation during the complex formation supports our idea of back flow of electron density to the σ^* ABMOs of the substituents of X group, i.e., towards C-F σ^* of $-\text{CF}_3$ group and N-O σ^* of $-\text{NO}_2$ group.

3.3 Population and Charge Analysis

Population density analysis at each of the scanned geometries gave information on influence of the long range exchange repulsion from Y-group to the electron density at the X-Hal σ^* ABMO. Results of Population analysis are shown in Fig. 6.

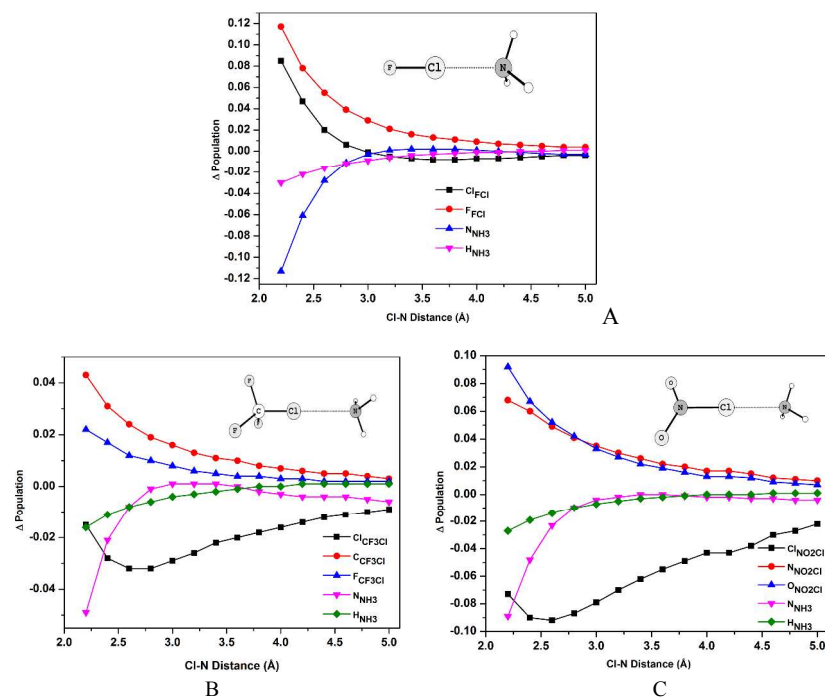


Fig. 6 Change in partial atomic population of the complex compared to the corresponding monomers during the scan: (A) $\text{FCl} \cdots \text{NH}_3$ (B) $\text{F}_3\text{CCl} \cdots \text{NH}_3$ (C) $\text{O}_2\text{NCl} \cdots \text{NH}_3$. Calculations are done at M06-2x/aug-cc-pVTZ level of theory.

The population of fluorine and chlorine atoms in $\text{F-Cl} \cdots \text{NH}_3$ complex is almost invariant at longer distances and increases as the donor-acceptor distance decreases (Fig. 6A). Both the donor and acceptor groups start reorganizing its electron population below 3.0 Å. This systematic change in population can be accounted by CT, which is largely a short range interaction. In contrast both Fig. 6(B) and Fig.

[journal], [year], [vol], 00–00 | 9

6(C) show that population of atoms in the halogen donor molecule changes even at longer distance where NH_3 population remain almost unchanged. This shows that even before NH_3 starts CT interaction with the donor molecule, the long range interactions begin. This reorganizes the electron density distribution of the halogen donor molecule. Analysis evidently shows that the halogen atom in the donor molecule loses electron density and the remaining portion of the molecule gains it. It can be observed from the Table 3 that, the incoming Y-group can reduce the magnitude of negative hyperconjugation that existed in the parent X-Z system and in addition force a negative hyperconjugative flow of electron density from the p-type lone pair on the chlorine atom to the ABMOs' of the X-group. Electron density from chlorine atom is shifted to the anti-bonding N-O orbital in $\text{O}_2\text{N-Cl}\cdots\text{NH}_3$ complex and towards anti-bonding C-F bond orbital in $\text{F}_3\text{C-Cl}\cdots\text{NH}_3$ complex. This type of intra-molecular stabilization is absent in the X-H bond (no extra orbitals and electrons on H). Therefore magnitude of blue-shift in H-bonded complexes will be much smaller than those in halogen and similar Z-bonds. Justification for the small blue-shift observed in $\text{CH}_3\text{Cl}\cdots\text{NH}_3$ ⁴⁶ complex can also be explained using the above arguments, where negative hyperconjugation to C-Cl σ^* ABMO in CH_3Cl is absent. The incoming NH_3 increases the extent of negative hyperconjugation from chlorine to C-H σ^* ABMO and hence increases the intra molecular interaction which leads to C-Cl bond length contraction. Thus in general, back flow of electron density leads to the generation of positive charge on the halogen atom which was slightly negatively charged in the monomer. The initial decrease in population density at chlorine atom in blue-shifted systems is a manifestation of the extend of the negative hyperconjugation that existed in the parent X-Z. This analysis shows the existence of long range exchange repulsive interaction which gets activated in Pro-improper Z-bonded systems. Immediate consequence of this is the redistribution of charge density in the X-Z molecule. In the case of $\text{F-Cl}\cdots\text{NH}_3$ (Red shifted) complex both F and Cl gain electron density during the approach of NH_3 . In $\text{F}_3\text{C-Cl}\cdots\text{NH}_3$ and $\text{O}_2\text{N-Cl}\cdots\text{NH}_3$ (blue-shift), Cl atom loses electron density and $-\text{CF}_3$ and $-\text{NO}_2$ groups gain electron density. It also shows that NH_3 does not lose any charge before it reaches a minimum distance (≈ 3.0 Å). Charge analysis also supports our arguments of long range exchange repulsion from Y and its consequence of intra molecular electron density reorganization in Z-bond donor molecule, without accepting any electron density from Y.

There exists a strong correlation between the nature of X-group, mode of σ -hole generation over Z-atom and negative hyperconjugation from X-group. Politzer et al⁴⁷⁻⁴⁹ proposed that the presence of a positive electrostatic potential region (σ hole) at the Z-atom is the reason for electrostatic attraction between monomers. The electronegativity of fluorine compared to chlorine in FCl makes the σ -hole in F-Cl molecule concentrated on the chlorine end. The σ hole in CH_3Cl is expected on the carbon end. However in CF_3Cl , the highly electron withdrawing fluorine substituents make carbon more electron demanding from chlorine, effectively increases the electronegativity of carbon as suggested by Mulliken and Jaffe.⁵⁰⁻⁵² Increased positive charge and hence increased electronegativity of carbon pulls electrons from chlorine atom and creates σ -hole at chlorine atom of C-Cl bond in CF_3Cl . This is reflected in the orbital coefficients of the σ^* MO of C-Cl bond (Fig 3). Larger lobe size at carbon atom of σ^* C-Cl bond helps to increase the negative hyperconjugation in the CF_3Cl , stretching the C-Cl bond than expected in its absence. Incoming NH_3 , decreases the negative hyperconjugation and hence more possibility for blue shifting

of C-Cl bond. Same effects can be observed in the case of O₂N-Cl molecule also. Thus larger electronegativity difference between the Z-atom and the connected atom of X-group, the larger will be the magnitude of negative hyperconjugation and consequently blue-shifting. The H-bonded complexes show lower magnitude in blue shifting due to the same reason.

3.4 Analysis of variation in electron density at Bond Critical Points during the complex formation

We have analysed the evolution of donor-acceptor system from monomers by carefully studying the position and properties of electron density at the bond critical points (BCP) during each scan steps. Analysing the position and topological properties⁵³ of BCPs' on either side of chlorine atom gives some defining parameters for characterizing red and blue-shifting bonds. The two bond critical points (red triangle and green dot) which are directly connected to the halogen atom are shown in Fig. 7

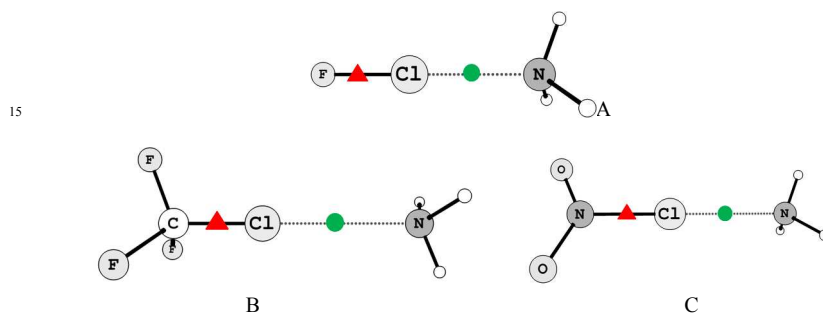
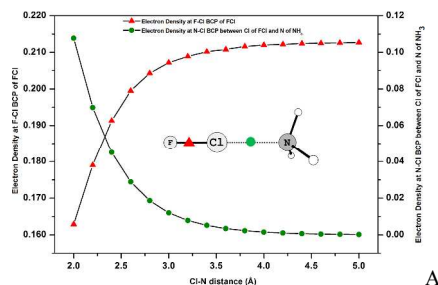


Fig. 7 Bond Critical Points (BCP) under investigation: (A) FCl---NH₃ (B) F₃CCl---NH₃ (C) O₂NCl--NH₃.

Red triangle represents the BCP at the X-Hal bond and the Green dot represents the BCP connecting the donor-acceptor system. Koch and Poplier⁵⁴ proposed eight criteria for characterizing H-bonds which are based on electron density at the BCP connecting donor and acceptor (green dot). Many studies showed that halogen bonds also follow some of those criteria. Systems studied here also agree with the density at BCP criteria (0.002a.u to 0.04a.u) but the Laplacian of density at BCP is slightly less than the predicted range for Hydrogen bonds (-0.15a.u to -0.02a.u). Analysis of electron density at both BCP for the three systems under our study is given in Fig. 8



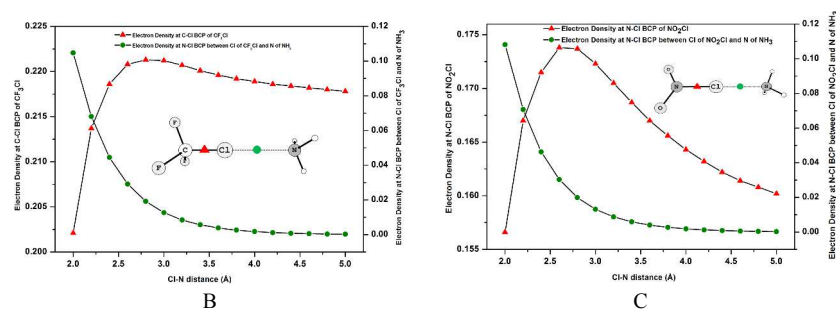
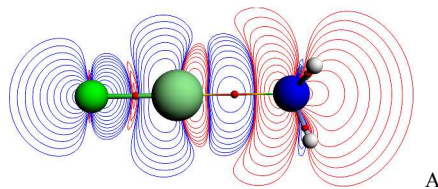


Fig. 8 Variation of electron density at BCPs on either side of Cl atom during scan: (A) FCl---NH₃ (B) F₃C-Cl---NH₃ (C) O₂N-Cl---NH₃. Calculations are done at MP2 optimized geometries.

5 Fig. 8A shows the characteristic electron density change in a normal red shifted system. Electron densities at both the BCPs are not changing at longer distances but starts changing when it reaches to the distance where CT begins. Decrease in electron density at F-Cl bond during the approach of NH₃ shows the nature of bond length elongation and extra electron occupancy at F-Cl σ^* orbital. Fig. 8B and 8C
 10 shows the characteristics of electron density change in blue-shifting bonds, where approach of Y-group removes extra electron density from σ^* X-Z bond orbital and hence electron density at the BCP increases. In the case of F₃C-Cl---NH₃ system, change in density at the C-Cl BCP is not so large and which can be correlated to the already explained population analysis and the σ^* occupation. The drastic decrease in
 15 N-Cl bond length during the formation of O₂N-Cl---NH₃ complex leads to the removal of extra electron density at the N-Cl σ^* ABMO. Hence the density curve sharply rises till the equilibrium geometry and then starts decreasing due to the larger CT form NH₃ lone pair. It can be seen that irrespective of the X-Z bond length change (as red- or blue-), density at the donor-acceptor interaction region is keep on
 20 increasing. This observation prompts us to propose that the weakly interacting complexes are formed not only because of the electrostatic attraction between the donor and acceptor but also due to the reorganization of electrons which binds the donor and acceptor molecule. Similar arguments were proposed by Grabowski about the covalent nature of H-bonded complexes based on QTAIM analysis.⁵⁵ Very
 25 recently Arunan et al. verified the covalency and ionicity of weakly interacting X-Z--Y complexes at the Z---Y region for Hydrogen, Halogen and Lithium bonds.³¹

Analysis of computational deformation density 2D contour maps also supports our argument of electron density reorganization as the reason for X-Z bond length variation during the complex formation. Deformation density gives information
 30 about the extent of electron density reorganization during the formation of the dimer from two separate monomers. Fig. 9 shows the deformation density contour maps at 0.0003 a.u isosurface. Red contours represent the electron density depleted region and the blue contours represent the electron density concentrated region.



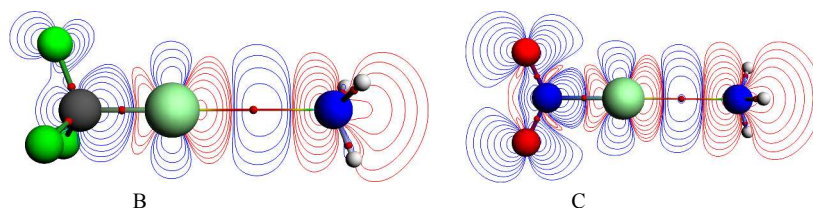


Fig. 9 2D Contour maps of the Deformation density at 0.0003 a.u. isosurface using equilibrium geometry: (A) FCl...NH₃ (B) F₃C-Cl...NH₃ (C) O₂N-Cl...NH₃. Calculations are done at M06-2x/TP2Z level of theory.

Fig. 9A shows the characteristic donation of lone pair on Y-group to the X-Z σ^* ABMO, where both Z-atom and X-group/atom receives electron density through charge transfer. Fig. 9B and 9C shows the electron density reorganized state of blue-shifting complexes, where electron density flows away from Z-atom and concentrated over X-group due to the long range exchange repulsion from Y-group on to the extra electron density at the σ^* ABMO. Electron density concentration in between the monomers represents the glue of electrons which holds X-Z and Y molecules. Though we have not discussed this explicitly, the variation in the position of the BCPs also follows from these arguments.

Now it is clear that, the negative hyperconjugation in X-Z molecule and extra electron occupancy at the X-Z σ^* orbital is the primary reason for the occurrence of pro-improper bonds in weakly interacting complexes and its absence leads to red shifting bonds. A few exceptions are known for this observation, e.g. CH₄...NH₃,²² where blue-shift in C-H bond length is observed even in the absence negative hyperconjugation. Such situations can be treated as the special cases of the generalized electron density reorganization mechanism. The negligible electronegativity difference between Hydrogen and Carbon atoms, where part of the electron density localized over the Hydrogen can easily be shifted towards the C-H bonding region by incoming Y-group, provides an exception. The applicability of the proposed concept and the inevitability of continuum nature of red- and blue-shifting bonds can be proved by analysing some well-studied weak interactions such as Hydrogen, Halogen, Chalcogen and Pnictogen Bonds.

4. On the continuum nature of weak interactions

Halogen bonded complexes discussed above are used as prototypical systems for understanding the interactions that govern the nature of weak X-Z...Y complexes. If the X-Z molecule does not have negative hyperconjugation from Z to X, the X-Z σ^* is likely to be more concentrated on the Z. This helps the flow of electrons from Y to X-Z σ^* . Hence we conclude that the absence of negative hyperconjugation from X-group to X-Z σ^* orbital in X-Z molecule leads to proper Z-bonds (red shift). On the other hand, presence of negative hyperconjugation from X-group to X-Z σ^* -orbital leads to red- or blue-shifting depending on the magnitude of hyperconjugation in X-Z. Thus the electron donating capacity of Y decides blue or red shift in the X-Z bond in X-Z...Y. These are called pro-improper Z-bonds. Computations on selected sets of complexes and literature data support these arguments (Table S1). Literature survey of four series of weakly interacting complexes- Hydrogen-bond, Halogen-bond, Chalcogen-bond, Pnictogen-bond, supports the above arguments. This, along

with the arguments developed in this article, allows the prediction of a continuum in weak interactions (Z-bonds) from red-, zero- and blue-shifting. This can be achieved by properly tuning the X- and Y-groups of the X-Z---Y complex. Fig. 10 shows the relative ordering of weakly interacting complexes based on the magnitude of X-Z bond length change and interaction energy. Halogen bonded complexes are found to be largely blue-shifted with lesser interaction energy, which is followed by Chalcogens, Hydrogens and Pnicogens.

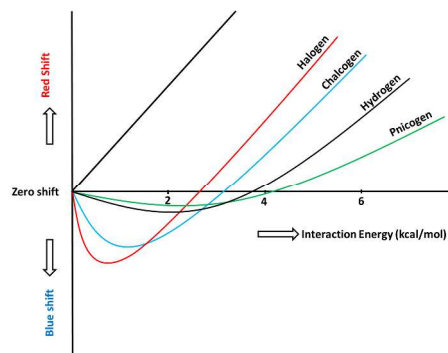


Fig. 10 A qualitative relationship between interaction energy and X-Z bond length change during the formation of different sets of weakly interacting complexes.

There exists a direct correlation between the interaction energy and equilibrium monomer separation. Studies showed that the major factors which decides the equilibrium geometry and hence interaction energy are the electrostatic attraction and the Pauli repulsion between the monomers along with polarization and dispersion components.^{12, 56} The electron density around the Z-atom of X-Z molecule decides the balance between these opposing forces. In the case of F-Cl molecule, higher electron withdrawing nature of F makes Cl atom electron deficient at the σ -hole direction. Consequent higher electrostatic attraction and lower Pauli repulsion lead to higher interaction energy and smaller monomer separation. This is not the case for CF_3Cl molecule. Here CF_3 - group electronegativity is only sufficient to make a weak σ -hole over Cl-atom. Thus larger electron density around the Cl atom creates higher Pauli repulsion and lower electrostatic attraction. This leads to lower interaction energy and larger monomer separations. Hence in general, blue-shifting halogen bonded complexes show lower interaction energy and higher monomer separations due to the higher electronegativity of the Z-atom compared to the connected atom of the X-group. Similar arguments can also be extended to Chalcogen, Pnicogen and Hydrogen bonded complexes (Table S2). Thus, based on the above premise we suggest that the equilibrium monomer separation and hence total interaction energy changes with variations in the effective charge density around the Z-atom.

Halogen bonded complexes show higher magnitude of X-Z bond length compression (blue-shifting). This can be inferred from the magnitude of negative hyperconjugation observed in these complexes. As explained above, higher electronegativity of Z-atom leads to larger MO coefficients at the X-atom which is directly connected to the Z-atom at the $\sigma^*\text{ABMO}$. This helps to increase the magnitude of electron density donation from its substituents through negative hyperconjugation. This increases the σ^* ABMO occupancy of X-Z bond and hence

the bond will be highly elongated in the monomer itself. The extra electron density at the σ^* orbital can easily be perturbed by the incoming Y-group which results in the shift of electron density from the anti-bonding MOs to where it came from (reversal of negative hyperconjugations). This leads to the X-Z bond compression and hence blue-shift. Thus, it can be concluded that, larger the electronegativity difference between the X- and Z- atoms, higher will be the extent of blue-shifting. This is the reason for lower magnitudes of blue-shifting in Hydrogen and Pnictogen bonded complexes compared to that of Halogen and Chalcogen bonded complexes, as implied in Fig. 10.

In general, red shifting bonds of varying interaction energy and bond length can be observed as shown in the upper portion of Fig. 10, for all Z atoms, but magnitude of blue-shifting and interaction energy are shown schematically for special characteristic features for each class of interactions. This essentially proves that, the proper selection of X- and Y- group for a particular class of Z- will eventually lead to X-Z---Y complexes with zero-shift in X-Z bond length and with non-zero interaction energy. This confirms the inevitability of a continuum of X-Z bond length change from red-, zero- and blue-shifting.

5. Conclusions

Extend of negative hyperconjugation and consequent lengthening of the X-Z bond in the parent Z-Bond donor differentiate the nature of proper and pro-improper in X-Z---Y complexes. The continuum nature of weak interactions from red-, zero- and blue-shifting has been analysed and correlated to the nature of X- and Y- groups along with the electron density around the Z-atom. Our understanding about the nature of X-Z---Y interactions and red- and blue-shifting X-Z bonds can be summarized as follows:

- (1) A new description for proper and pro-improper bonds has been given; monomers with no negative hyperconjugation mostly falls in the category of proper (red-shifting) and those with negative hyperconjugation falls in the category of pro-improper (red- or blue-shifting).
- (2) A direct correlation exists between total interaction energy and the monomer separation at the equilibrium geometry, which is decided by the electron density around the Z-atom.
- (3) The magnitude of blue-shifting depends on the electronegativity difference between the Z-atom and the X-group atom connected to Z. Larger the electronegativity difference, larger will be the negative hyperconjugation and hence larger blue-shifting.
- (4) The continuum nature of weak interactions from red-, zero- and blue-shifting can be applied to any X-Z---Y complex. It is decided by the composite of the magnitudes of σ -hole and negative hyperconjugation from X-group, and the exchange repulsion and charge transfer from the Y-group, the variation of the individual magnitudes estimated as mentioned above.

Acknowledgements

The authors thank IISER-TVM, IISc-Bangalore and CMSD-Hyderabad for computational facilities. EDJ Thanks the DST for funding through the J. C. Bose

Fellowship. JJ and KV thank UGC-India for Senior Research Fellowship.

References

1. G. R. Desiraju and T. Steiner, *The weak hydrogen bond : In structural chemistry and biology*, Oxford University Press, Oxford ; New York, 1999.
- 5 2. G. A. Jeffrey and W. Saenger, *Hydrogen bonding in biological structures*, Student edn., Springer-Verlag, Berlin ; New York, 1994.
3. S. Srivastava, *Recent development in material science*, 1st edn., Research India Press, New Delhi, 2011.
4. E. R. T. Tiekink, J. J. Vittal and M. Zaworotko, *Organic crystal engineering : frontiers in crystal engineering*, Wiley, Chichester, U.K., 2010.
- 10 5. E. Arunan, *Curr. Sci.*, 2013, **105**, 892-894.
6. W. Wang, N.-B. Wong, W. Zheng and A. Tian, *J. Phys. Chem. A*, 2004, **108**, 1799-1805.
7. W. Wang and P. Hobza, *J. Phys. Chem. A*, 2008, **112**, 4114-4119.
8. C. Wang, D. Danovich, Y. Mo and S. Shaik, *J. Chem. Theory Comput.*, 2014, **10**, 3726-3737.
- 15 9. J. Fanfrlík, A. Práda, Z. Padělková, A. Pecina, J. Macháček, M. Lepšík, J. Holub, A. Růžička, D. Hnyk and P. Hobza, *Angew. Chem., Int. Ed.*, 2014, **53**, 10139-10142.
10. R. Gleiter and G. Haberhauer, *J. Org. Chem.*, 2014, **79**, 7543-7552.
11. S. Zahn, R. Frank, E. Hey-Hawkins and B. Kirchner, *Chem. Eur. J.*, 2011, **17**, 6034-6038.
- 20 12. S. Scheiner, *Int. J. Quantum Chem.*, 2013, **113**, 1609-1620.
13. A. Bauzá, T. J. Mooibroek and A. Frontera, *Angew. Chem., Int. Ed.*, 2013, **52**, 12317-12321.
14. D. Mani and E. Arunan, *Phys. Chem. Chem. Phys.*, 2013, **15**, 14377-14383.
- 25 15. S. J. Grabowski, *Phys. Chem. Chem. Phys.*, 2014, **16**, 1824-1834.
16. W. Wang, Y. Zhang, B. Ji and A. Tian, *J. Chem. Phys.*, 2011, **134**, 224303-224308.
17. B. Ji, Y. Zhang, D. Deng and W. Wang, *CrystEngComm*, 2013, **15**, 3093-3096.
18. B. Raghavendra and E. Arunan, *J. Phys. Chem. A*, 2007, **111**, 9699-9706.
19. W. Zierkiewicz, D. Michalska, Z. Havlas and P. Hobza, *ChemPhysChem*, 2002, **3**, 511-518.
- 30 20. S. Scheiner, S. J. Grabowski and T. Kar, *J. Phys. Chem. A*, 2001, **105**, 10607-10612.
21. B. J. van der Veken, W. A. Herrebout, R. Szostak, D. N. Shchepkin, Z. Havlas and P. Hobza, *J. Am. Chem. Soc.*, 2001, **123**, 12290-12293.
22. Y. Gu, T. Kar and S. Scheiner, *J. Am. Chem. Soc.*, 1999, **121**, 9411-9422.
- 35 23. W. Qian and S. Krimm, *J. Phys. Chem. A*, 2002, **106**, 6628-6636.
24. I. V. Alabugin, M. Manoharan, S. Peabody and F. Weinhold, *J. Am. Chem. Soc.*, 2003, **125**, 5973-5987.
25. I. V. Alabugin, S. Bresch and M. Manoharan, *J. Phys. Chem. A*, 2014, **118**, 3663-3677.
26. J. Joseph and E. D. Jemmis, *J. Am. Chem. Soc.*, 2007, **129**, 4620-4632.
- 40 27. P. Hobza, V. Špirko, H. L. Selzle and E. W. Schlag, *J. Phys. Chem. A*, 1998, **102**, 2501-2504.
28. P. Hobza and Z. Havlas, *Chem. Rev.*, 2000, **100**, 4253-4264.
29. M. J. Frisch, G. W. Trucks, H. B. Schlegel, G. E. Scuseria, M. A. Robb, J. R. Cheeseman, G. Scalmani, V. Barone, B. Mennucci, G. A. Petersson, H. Nakatsuji, M. Caricato, X. Li, H. P. Hratchian, A. F. Izmaylov, J. Bloino, G. Zheng, J. L. Sonnenberg, M. Hada, M. Ehara, K. Toyota, R. Fukuda, J. Hasegawa, M. Ishida, T. Nakajima, Y. Honda, O. Kitao, H. Nakai, T. Vreven, J. A. Montgomery, J. E. Peralta, F. Ogliaro, M. Bearpark, J. J. Heyd, E. Brothers, K. N. Kudin, V. N. Staroverov, R. Kobayashi, J. Normand, K. Raghavachari, A. Rendell, J. C. Burant, S. S. Iyengar, J. Tomasi, M. Cossi, N. Rega, J. M. Millam, M. Klene, J. E. Knox, J. B. Cross, V. Bakken, C. Adamo, J. Jaramillo, R. Gomperts, R. E. Stratmann, O. Yazyev, A. J. Austin, R. Cammi, C. Pomelli, J. W. Ochterski, R. L. Martin, K. Morokuma, V. G. Zakrzewski, G. A. Voth, P. Salvador, J. J. Dannenberg, S. Dapprich, A. D. Daniels, Farkas, J. B. Foresman, J. V. Ortiz, J. Cioslowski and D. J. Fox, *Gaussian, Inc.*, Wallingford CT, 2010.
- 50 30. C. Bleiholder, D. B. Werz, H. Köppel and R. Gleiter, *J. Am. Chem. Soc.*, 2006, **128**, 2666-2674.
31. A. Shahi and E. Arunan, *Phys. Chem. Chem. Phys.*, 2014, **16**, 22935-22952.
32. S. Grimme, J. Antony, S. Ehrlich and H. Krieg, *J. Chem. Phys.*, 2010, **132**, 1-19.

33. L. Goerigk and S. Grimme, *J. Chem. Theory Comput.*, 2010, **7**, 291-309.
34. S. F. Boys and F. Bernardi, *Mol. Phys.*, 1970, **19**, 553-566.
35. G. te Velde, F. M. Bickelhaupt, E. J. Baerends, C. Fonseca Guerra, S. J. A. van Gisbergen, J. G. Snijders and T. Ziegler, *J. Comput. Chem.*, 2001, **22**, 931-967.
- 5 36. J. B. Biegler-König F.; Schönbohm, *J. Comput. Chem.*, 2001, **22**, 545-559.
37. M. Mitoraj and A. Michalak, *J. Mol. Model.*, 2007, **13**, 347-355.
38. T. Ziegler and A. Rauk, *Inorg. Chem.*, 1979, **18**, 1755-1759.
39. E. D. Glendening, C. R. Landis and F. Weinhold, *J. Comput. Chem.*, 2013, **34**, 1429-1437.
- 10 40. S. M. Huber, J. D. Scanlon, E. Jimenez-Izal, J. M. Ugalde and I. Infante, *Phys. Chem. Chem. Phys.*, 2013, **15**, 10350-10357.
41. P. Politzer, J. S. Murray and T. Clark, *Phys. Chem. Chem. Phys.*, 2010, **12**, 7748-7757.
42. M. D. Esrafilii and B. Ahmadi, *Comp. Theor. Chem.*, 2012, **997**, 77-82.
43. I. Fleming, *Molecular orbitals and organic chemical reactions*, Student edn., Wiley, Chichester, West Sussex, U.K., 2009.
- 15 44. A. D. McNaught and A. Wilkinson, *Compendium of chemical terminology : IUPAC recommendations*, 2nd edn., Blackwell Science, Oxford England ; Malden, MA, USA, 1997.
45. A. Obermeyer, H. Borrmann and A. Simon, *J. Am. Chem. Soc.*, 1995, **117**, 7887-7890.
- 20 46. J.-W. Zou, Y.-J. Jiang, M. Guo, G.-X. Hu, B. Zhang, H.-C. Liu and Q.-S. Yu, *Chem. Eur. J.*, 2005, **11**, 740-751.
47. T. Clark, M. Hennemann, J. Murray and P. Politzer, *J. Mol. Model.*, 2007, **13**, 291-296.
48. P. Politzer, J. S. Murray and P. Lane, *Int. J. Quantum Chem.*, 2007, **107**, 3046-3052.
49. P. Politzer, J. S. Murray and T. Clark, *Phys. Chem. Chem. Phys.*, 2013, **15**, 11178-11189.
- 25 50. R. S. Mulliken, *J. Chem. Phys.*, 1934, **2**, 782-793.
51. J. Hinze and H. H. Jaffe, *J. Am. Chem. Soc.*, 1962, **84**, 540-546.
52. J. Hinze, M. A. Whitehead and H. H. Jaffe, *J. Am. Chem. Soc.*, 1963, **85**, 148-154.
53. R. F. W. Bader, *Atoms in molecules : a quantum theory*, Clarendon Press, Oxford ; New York, 1990.
- 30 54. U. Koch and P. L. A. Popelier, *J. Phys. Chem.*, 1995, **99**, 9747-9754.
55. S. J. Grabowski, *Chem. Rev.*, 2011, **111**, 2597-2625.
56. D. R. Duarte, G. Sosa and N. Peruchena, *J. Mol. Model.*, 2013, **19**, 2035-2041.